ACSNANO
www.acsnano.org
ARTICLE

Formation of Ordered Coronene Clusters in Template Utilizing the Structural Transformation of Hexaphenylbenzene Derivative Networks on Graphite Surface

Shaoqing Chang,[†] Runcong Liu,[‡] Liancheng Wang,[§] Min Li,*[,‡] Ke Deng,*[,†] Qiyu Zheng,*[,§] and Qingdao Zeng*[,†]

[†]CAS Key Laboratory of Standardization and Measurement for Nanotechnology, CAS Center for Excellence in Nanoscience, National Center for Nanoscience and Technology (NCNST), Beijing 100190, P. R. China

[‡]CAS Key Laboratory for Biomedical Effects of Nanomaterials and Nanosafety, Institute of High Energy Physics, Chinese Academy of Sciences, Beijing 100049, P. R. China

[§]Beijing National Laboratory for Molecular Sciences, CAS Key Laboratory of Molecular Recognition and Function, Institute of Chemistry, Chinese Academy of Sciences, Beijing, 100190, P. R. China

Supporting Information

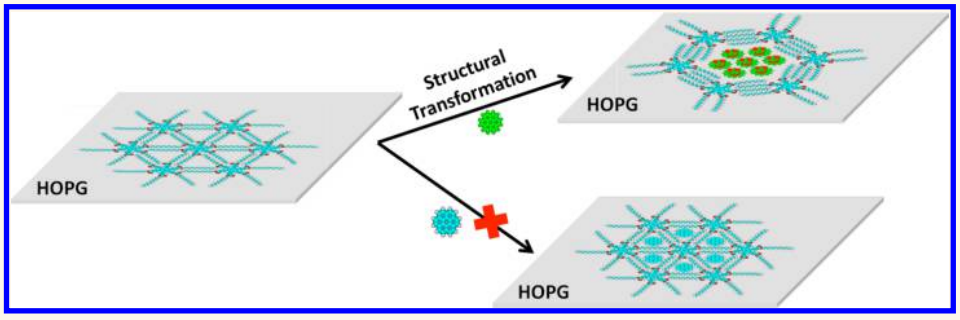

ABSTRACT: **In the present work, we report the fabrication of regular coronene (COR) clusters on surfaces in ambient conditions in the two-dimensional network formed by hexaphenylbenzene derivatives (HPB) via structural transformation. HPB could form a stable snowflake network structure on the highly oriented pyrolytic graphite surface at the air−solid interface. When COR molecules were introduced into the system, the HPB snowflake network could transform to honeycomb structures, and the COR heptamers were subsequently aggregated and entrapped into the cavity. Scanning tunneling microscopic was employed to monitor the assembly behavior of both HPB and HPB/COR at a submolecule scale level, and density functional theory calculations were utilized to reveal that the structural transformation and the entrapment are the energetically favorable. The pores formed from HPB might also give a clue to immobilizing some functional molecule clusters, like COR, to fabricate their ordered monolayer in ambient conditions, so as to obtain complex supramolecular surface structures.**

KEYWORDS: *structural transformation, HPB network, coronene cluster, scanning tunneling microscopy, guest inclusion*

Self-assembly of functional molecules at surfaces and interfaces is of great significance in supramolecular chemistry. Among those, well-ordered two-dimensional (2D) networks have received a lot of attention due to their broad range of potential applications, *i.e.*, immobilization and isolation of functional objects as a guest unit at the molecular scale.[1−6] Design and formation of the regular pattern of functional molecule clusters on surfaces is of interest from both scientific and technological viewpoints. Coronene (COR) can be regarded as a smaller graphene fragment but without the disadvantages of irregular shapes and variable sizes of graphene sheets.[7,8] This molecule is considered to be a suitable candidate for the component of molecular rotors due to its π-conjugated and highly symmetric molecular structure.[9] Specifically, COR-like clusters or aggregates, as an important carbon-based material, have received a lot of attention in electronic devices due to their unique electronic properties derived from the perfect delocalization of the aromaticity among the six outer

Received: July 31, 2015
Accepted: December 8, 2015
Published: December 9, 2015

DOI: 10.1021/acsnano.5b06666
ACS Nano 2016, 10, 342−348

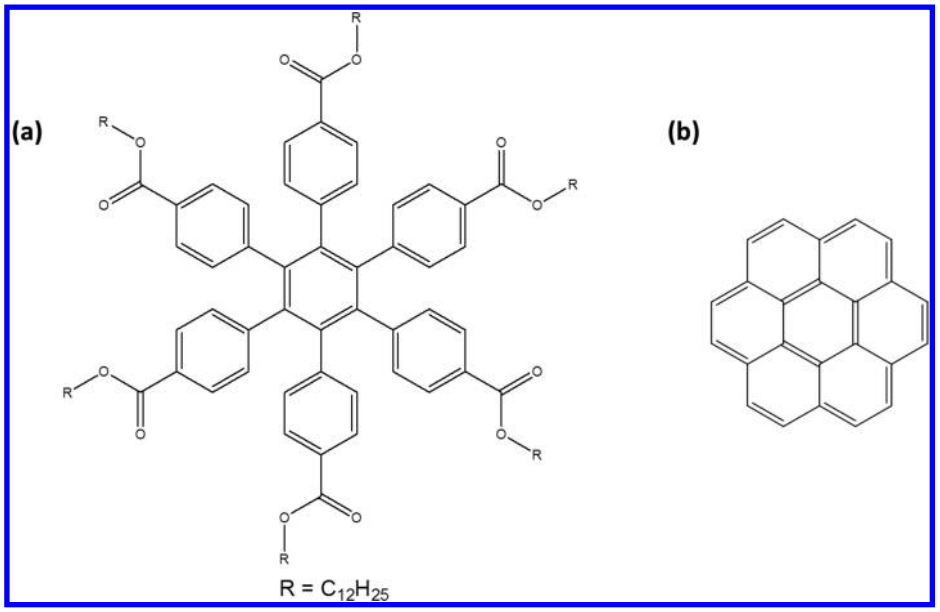

Figure 1. Chemical structures of the (a) HPB and (b) COR.

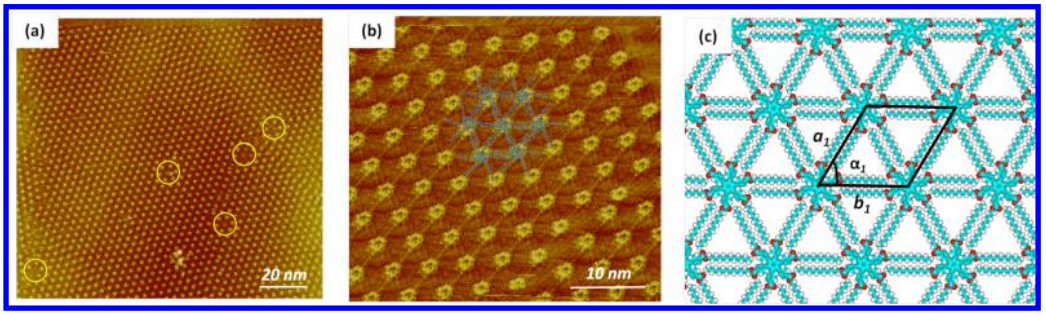

Figure 2. (a) Large-scale and (b) high-resolution STM images of the snowflake-like structures. The scanning conditions are I = 296 pA, V = 595 mV. (c) Calculated molecular model for this assembly obtained from DFT simulations (C, cyan; O, red; H, gray). Note: In order to clearly display the calculated molecular models, HOPG surfaces are not shown.

rings.[10] This kind of structure is, however, difficult to construct on the surface, owing to the harsh conditions required, *i.e.*, large network cavity, strong interaction between clusters and substrate/network. Rare work has been reported to successfully construct patterned molecular clusters on surfaces.[1,6] Noncovalent interactions are widely exploited in obtaining 2D assembly network structures which were used as the templates to immobilize or isolate molecular rows, clusters, or big molecular circles as well as more complex multicomponent arrangements.[1,11−14] Both rigid molecular networks with permanent porosities and flexible networks have been reported to successfully immobilize functional target molecules especially under ultrahigh vacuum conditions. In contrast, less work has been done on flexible networks which can involve a conformational change on adsorption or the pronounced structural transformation in response to environmental change including guest inclusion.[15−18] This kind of network would provide high guest selectivity, for example, flat molecules containing large π-conjugated moieties or buckyball structure-like fullerene. The diversity of the supramolecular network makes it not only capable of serving as the template to trap guest molecules but also able to form functional molecular aggregation or supramolecular structure.[1,6,13] Therefore, the design and tuning of supramolecular nanostructure is of great theoretical and practical importance. Study of the structural change in the assemblies in response to guest inclusion could lead to a better comprehension of the concept of competitive adsorption for the fabrication of functional molecular arrays. Specifically, scanning tunneling microscopy (STM) is a strong tool to investigate the dynamics of guest trapping, diffusion, and manipulation in/on these host networks.[19−22]

In this work, we employed STM and studied the assembly behavior of hexaphenylbenzene derivatives (HPB) molecules on a highly oriented pyrolytic graphite (HOPG) surface and then successfully constructed the regular pattern of COR clusters in ambient conditions via the structural transformation of this template. STM measurements and density functional theory (DFT) calculations were utilized to reveal the reconstruction phenomenon of a 2D nanoporous network induced by a co-adsorbed guest molecule.

RESULTS AND DISCUSSION

HPB molecule, based on its molecular structure shown in Figure 1a, is a large π-conjugate system with high electronic state density. It is a derivative of the chemical studied in our previous work and could also form similarly assembled structure on a HOPG surface.[23] Figure 2a is a large-scale STM image that shows the assembly of HPB molecules when adsorbing onto HOPG surface. More details of the molecular structure are revealed by high-resolution image shown in Figure

DOI: 10.1021/acsnano.5b06666
ACS Nano 2016, 10, 342−348

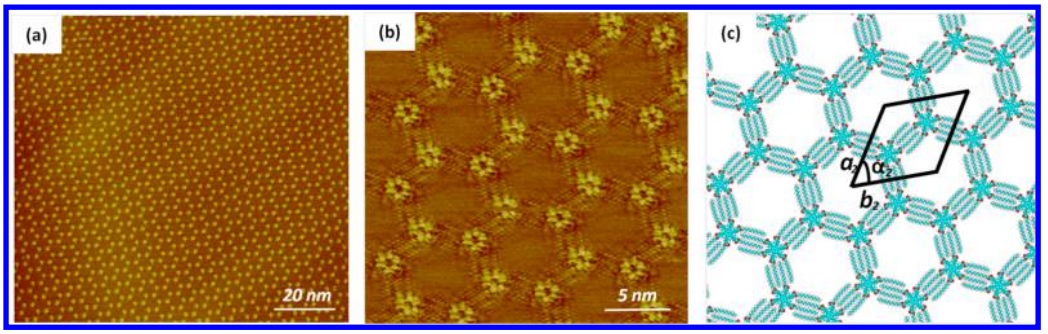

Figure 3. (a) Large-scale and (b) high-resolution STM images of the honeycomb structure (c).Calculated molecular model for this assembly obtained from DFT simulations (C, cyan; O, red; H, gray). Note: In order to clearly display the calculated molecular models, HOPG surfaces are not shown.

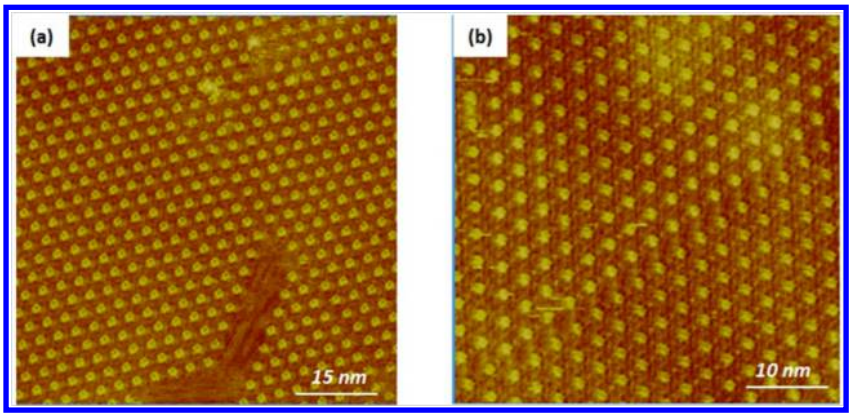

Figure 4. (a) STM image of HPB molecule after the samples were diluted by 10 times (I = 299 pA, V = 699 mV). (b)STM image of HPB molecule after the samples were diluted by 500 times (I = 299 pA, V = 699 mV).

2b. The bright circle in Figure 2b corresponds to the conjugated backbone of HPB molecule.

The circle center presents a low-contrast feature, possibly due to the fact that the peripheral benzene rings tend to rotate by a certain angle from the central plane to decrease the steric hindrance, and accordingly the peripheral benzene rings are higher than the central benzene ring. The diameter of the circle is around 1.5 nm, which is consistent with the observation reported in our previous work.[23] The thin lines linking these circles in the darker area are attributed to the alkyl chains. The alkyl chains of HPB molecules are fully stretched, which is proved by the fact that the length of the alkyl chains determined from the STM images is 1.6 ± 0.1 nm, fitting the length of alkyl chain with 12 carbons. The size of the triangular cavity formed in the assembly is about 1.2 nm (length of the edge of the triangle). The suggested molecular model based on the STM observation is given in Figure 2c, with the unit cell: $a_1 = b_1$ = 3.1 ± 0.1 nm and α_1 = 60 ± 1.0°.

Besides the snowflake structure, honeycomb structure was also occasionally observed in our experiments, as shown in Figure 3. It should be noted that this structure could still be observed in the snowflake pattern (marked by circles where we call it defects), as shown in Figure 2, which appears mostly in phase boundary. The high-resolution image was shown in Figure 3b. Each bright spot corresponds to the central backbone of a HPB molecule. And six HPB molecules form into a honeycomb unit cell with a central pore size of 4.0 ± 0.1 nm in diameter. It is clear that all six alkyl chains of a HPB molecule are fully stretched. Different from the structure of HPB in the snowflake assembly, every two adjacent alkyl chains are paired into three groups, which are evenly distributed around the central backbone. In each group, the paired alkyl chains were parallel in the same direction. Subsequently, one HPB molecule could interact with the adjacent HPB molecule through the opposite pairs of alkyl chains. The parameters of the cell unit determined from the STM images were addressed in Figure 3c with $a_2 = b_2$ = 5.5 ± 0.1 nm and α_2 = 60 ± 1.0°.

It is worth mentioning that there is a low possibility of observing this honeycomb structure, and even when it appears in the detection area, it soon disappears during scanning. This indicates that such structure is unstable, possibly a transition state during the assembling process. However, it is very attractive to be characteristic with such large cavities (4.0 nm) on surfaces in ambient conditions, being of great potential to the formation of clusters from small functional molecules, for example, COR molecules. To obtain this structure, one possible way is to decrease the sample concentration if the assembling behavior of HPB on HOPG is dependent on the concentration.

The next experiments were performed on the sample with a diluted solution to check the network stability upon concentration. The same 2D snowflake structure is observed as shown in Figure 4a when diluting the sample solution used in Figure 2 by 10 times. We then further diluted the solution by 500 times and found that the assembled structure stays the same as presented in Figure 4b. It should be noted that for both cases of the diluted samples, the HOPG surface was observed with the snowflake structure in all detectable areas within the experimental range, suggesting that concentration does not significantly affect the assembling behavior of HPB molecules. It implies that the interaction between HPB molecules and the

DOI: 10.1021/acsnano.5b06666
ACS Nano 2016, 10, 342−348

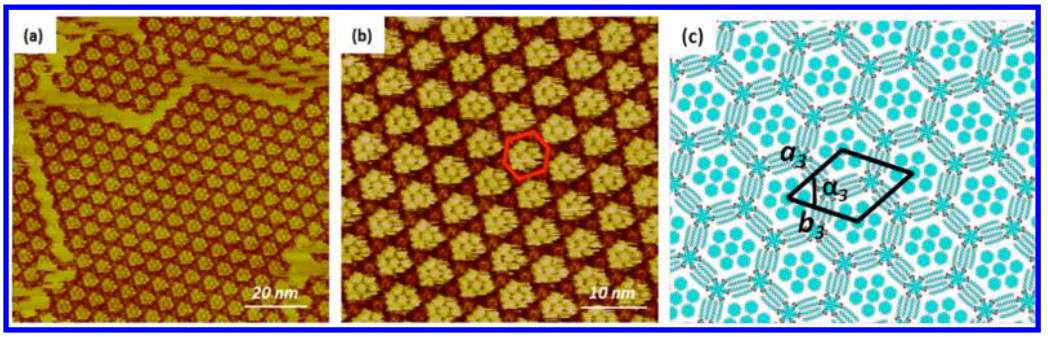

Figure 5. (a) Large-scale STM image of the HPB-COR co-adsorbed on the HOPG surface (I = 217 pA, V = 600 mV). (b) High-resolution image of HPB-COR co-adsorption assembly (I = 217 pA, V = 600 mV). (c) Calculated molecular model for this assembly obtained from DFT simulations (C, cyan; O, red; H, gray). Note: In order to clearly display the calculated molecular models, HOPG surfaces are not shown.

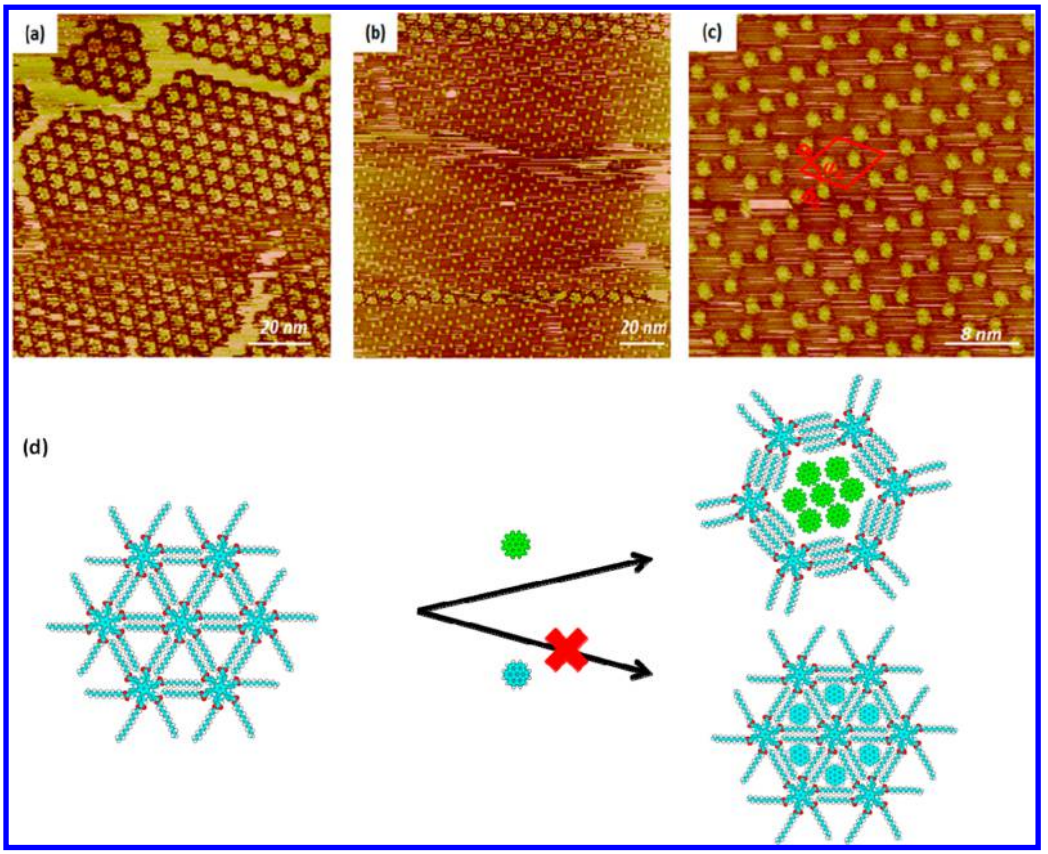

Figure 6. (a) Large-scale STM image of the HPB networks modulated by COR on HOPG surface (I = 299 pA, V = 699 mV). (b) Large-scale STM image of the template structure after removing COR (I = 299 pA, V = 699 mV). (c) High-resolution STM image of the template structure after removing COR. (d) Tentative models of the surface patterns of capturing at most seven COR molecules (C, cyan; O, red; H, gray). Note: In order to clearly display the calculated molecular models, HOPG surfaces are not shown.

graphene networks is determinant for determining the final assembly structure. These results also give a clue that the honeycomb structure shown in Figure 3 is not a consequence of the lower concentration of the sample.

It is interesting that HPB assemblies could yield larger pores and thus are capable of serving as traps for the inclusion of several large molecules. We demonstrate this potential by introducing COR to the network. As shown in Figure 5a, which shows an STM image acquired after deposition of COR, heptameric COR clusters have a compact hexagonal arrangement within the pores. The aggregate involving seven bright spots can be clearly identified in each pore, with the diameter of each bright spot of around 1.0 nm (Figure 5b). The size of the bright spot matches well with that of COR molecule. This is different from the case of its derivative HPB-6pa,[23] where the introduced COR molecules assemble into a honeycomb supramolecular structure on top of the HPB-6pa monolayer instead of entrapping in the cavity. This could be due to the capability of HPB to form much larger pores after structural transformation upon COR's inclusion. The parameters of the unit cell for this binary assembly structure are determined based on STM observations with $a_3 = b_3 = 5.5 \pm 0.1$ nm and $\alpha_3 = 60 \pm 1.0°$ (Figure 3c) and fits well with the honeycomb structure of HPB (Figure 3). It is plausible to suggest that when introducing COR into a HPB system, the assembly undergoes a dramatic transformation from the snowflake structure to the

DOI: 10.1021/acsnano.5b06666
ACS Nano 2016, 10, 342−348

honeycomb structure, and COR molecules aggregate into heptamers to be entrapped in the cavities of the honeycomb template of HPB. Further control experiments have been performed to confirm the conjecture. We adjusted the scanning conditions (reducing the distance between STM tip and substrate by applying a high set point value) to remove the above COR molecules. The acquired images are shown in Figure 6b,c. Obviously, the assembly is the honeycomb structure instead of the snowflake structure and serves as a template and traps COR clusters into its pores. The unit cell of the honeycomb structure was also measured in this case as marked in Figure 6c, with parameters of $a_4 = b_4 = 5.5 \pm 0.1$ nm and $\alpha_4 = 60 \pm 1.0°$, which is the same to that of the honeycomb structure in the absence of COR molecules (Figure 3). The results confirm the conclusion that the structural transformation is successfully achieved from snowflake to honeycomb network in response to COR guest inclusion.

To better understand and control the self-assembled architecture of HPB network, simulation was performed by DFT calculations. The calculated lattice parameters for 2D networks are summarized in Table 1. The cell size, the structures, and the geometry of the adsorbates are presented in the Supporting Information (see SI). The calculated parameters agree well with the experimental data. We present the total energy (including the interaction between adsorbates and the interaction between adsorbates and substrate) for the different assemblies in Table 2. Generally, we could compare the total energy to evaluate the thermodynamic stability of the different systems with the same unit cell. However, we should consider the effect of the unit area when comparing two systems with different unit cells. For the system with the smaller unit cell, there should be more molecules adsorbed on the substrate within the same area and subsequently contribute more energy to the whole system. Therefore, we presented the total energy per unit area to compare the thermodynamic stability of the different arrays to avoid such effect. The total energies per unit area of the different systems are also listed in Table 2. It should be mentioned that besides DFT calculations, the DFT-D3 method was also employed in our work. Considering that the interaction between adsorbates and substrate is mainly van der Waals interaction, the dispersion corrections (for example, the Grimme's dispersion corrections) should be included in the results. Although the absolute energy interaction is strongly dependent on the functional type employed in DFT, the interactions calculated by different functionals are with the similar trend.

Table 1. Experimental (expt) and Calculated (calcd) Lattice Parameters for the 2D Networks

		unit cell parameters		
		a (nm)	b (nm)	α (deg)
HPB-snowflake	expt	3.1 ± 0.1	3.1 ± 0.1	60 ± 1.0
	calcd	3.12	3.12	60.00
HPB-honeycomb	expt	5.5 ± 0.1	5.5 ± 0.1	60 ± 1.0
	calcd	5.47	5.47	60.00
HPB-honeycomb/COR7	expt	5.5 ± 0.1	5.5 ± 0.1	60 ± 1.0
	calcd	5.47	5.47	60.00

In Table 2, the interactions (DFT) between adsorbates of HPB-snowflake and HPB-honeycomb structures are −24.458 and −66.835 kcal·mol^{-1}, respectively, which mainly come from the 2D crystallization among alkyl chains of HPB molecules. We notice that both DFT and DFT-D3 results show that the interactions between adsorbates and substrate are very strong. Due to the inclusion of dispersion forces, the interactions between adsorbates and substrate by DFT-D3 method are lower than those by the conventional DFT method. Detailed analyses reveal that a 21% contribution to the interactions between adsorbate and substrate comes from the strong $\pi-\pi$ interaction between the central benzene ring of HPB and HOPG. And both the HPB-snowflake and the HPB-honeycomb structures are mainly stabilized by the van der Waals interaction between the alkyl chains of HPB molecules and HOPG. Therefore, the alkyl chains of HPB molecules play a pivotal role in forming the final assembly. Though the total energy of the HPB-snowflake structure is nearly half of that of the HPB-honeycomb structure, the total energy per unit area of the HPB-snowflake structure is much lower than that of HPB-honeycomb structure because of its much smaller unit area. It indicates that the HPB-snowflake structure is much more stable than the HPB-honeycomb structure. This is why we could observe the HPB-snowflake assembly in a large scale, while the HPB-honeycomb assembly recorded occasionally on the boundary.

It is noteworthy that the HPB-honeycomb network is with the large cavities (4.0 nm), which is commensurate with the heptameric COR clusters (with the whole size of 3.6 nm). In addition, due to their large planar π-conjugated cores, COR molecules could strongly interact with graphite. Thus, when COR molecules are introduced into the HPB system, they would be easily included into the cavities of HPB-honeycomb network. On the contrary, although the size of the triangular cavity (1.2 nm) is larger than the diameter of COR (1.0 nm), the interaction between the HPB-snowflake and COR presents a strong repulsion (129.736 kcal mol^{-1} by DFT method, 196.217 kcal mol^{-1} by DFT-D3 method) so that COR could not be stably inserted into the HPB-snowflake network. The total energy per unit area of HPB-honeycomb/COR7 could present the quantitative evidence. HPB-honeycomb/COR7 is with the lowest total energy per unit area (−0.288 kcal mol^{-1} Å^{-2} by DFT method, −0.395 kcal mol^{-1} Å^{-2} by DFT-D3

Table 2. Total Energy and the Energy Per Unit Area for Adsorbates on the HOPG Surface with DFT and DFT-D3 Methods[a]

	interactions between adsorbates (kcal mol^{-1})		interactions between adsorbates and substrate (kcal mol^{-1})		total energy (kcal mol^{-1})		total energy per unit area (kcal mol^{-1} Å^{-2})	
method	DFT	DFT-D3	DFT	DFT-D3	DFT	DFT-D3	DFT	DFT-D3
HPB-snowflake	−24.458	−4.699	−212.336	−296.477	−236.794	−301.176	−0.281	−0.357
HPB-honeycomb	−66.835	−46.513	−426.283	−571.950	−493.118	−618.463	−0.190	−0.239
HPB-honeycomb/COR7	−68.448	−47.258	−677.535	−976.991	−745.983	−1024.249	−0.288	−0.395

[a]The total energy includes the interaction energy between adsorbates and the interaction energy between adsorbates and the substrate. The more negative energy means the system is more stable

DOI: 10.1021/acsnano.5b06666
ACS Nano 2016, 10, 342−348

method), which means it is the most energetically favorable structure. Therefore, when COR molecules are introduced into the system, the snowflake structure could not trap any COR molecules into the triangular cavity, but transforms to the honeycomb network. Meanwhile, the COR molecules aggregate to a heptamer (named COR7). In the presence of the strong interaction between COR and substrate and with the matching size to the cavity of HPB honeycomb structure, the COR heptamer could be entrapped into the networks.

CONCLUSION

In conclusion, by means of STM technique and DFT simulation, we investigated the assembly behavior of HPB molecules on HOPG surface. Once depositing a droplet of HPB on HOPG surface, HPB-snowflake structure was observed in a large scale by STM technique. Besides the snowflake structure, honeycomb structure was also occasionally observed. When introducing COR molecules, for the first time, we observed the fabrication of regular COR clusters in the 2D HPB network via structural transformation of the host network from the snowflake to honeycomb structure. DFT calculations as well as the DFT-D3 calculations reveal that HPB-snowflake structure is more stable than HPB-honeycomb structure. However, COR molecules could aggregate into the cavity of the honeycomb structure to form COR7 cluster, and such an assembly is the most energetically favorable structure. These results give us an improved understanding of the interactions between guest molecules and the template as well as the substrate and encourage us to construct new functional assemblies by utilizing the advantages of the host−guest combination. The pores formed from HPB might also give a clue to immobilizing some functional molecule clusters, like COR, to fabricate their ordered monolayer in ambient conditions, so as to obtain complex supramolecular surface structures.

METHODS

HPB compound was synthesized according to the reported method.[23] Toluene was purchased from Acros Co. and used without further purification. COR was obtained from Sigma-Aldrich. The chemical structures of HPB and COR are shown in Figure 1.

HPB was dissolved in toluene at a concentration of 10^{-4} M. The samples were prepared by depositing a droplet of the above solution on a basal plane of a freshly cleaved HOPG (provided by ZYB, NT-MDT, Russia) surface. The samples were then annealed in an oven at either 60 or 100 °C, respectively, for 10 min. For host−guest system, a droplet of COR solution (in toluene) was added into the previously formed HPB network at room temperature prior to imaging. STM experiments were carried out with a Nano IIIa scanning probe microscope system (Bruker, USA) in ambient conditions. Tips were mechanically cut from Pt/Ir(80/20) wires. All STM images were recorded in the constant current mode. Detailed scanning parameters are provided in the caption of each image.

Theoretical calculations were performed using DFT provided by DMol^3 code.[24] We used the periodic boundary conditions (PBC) to describe the 2D periodic structure on the graphite in this work. The Perdew and Wang parametrization of the local exchange−correlation energy was applied in local spin density approximation to describe exchange and correlation.[25] All-electron spin-unrestricted Kohn−Sham wave functions were expanded in a local atomic orbital basis. For the large system, the numerical basis set was applied. All calculations were all-electron ones and performed with the medium mesh. Self-consistent field procedure was done with a convergence criterion of 10^{-5} au on the energy and electron density. Combined with the experimental data, we optimized the unit cell parameters and the geometry of the adsorbates in the unit cell. When the energy and density convergence criterion were reached, we could obtain the optimized parameters and the interaction energy between adsorbates.

To evaluate the interaction between the adsorbates and HOPG, we designed the model system. In our work, since adsorption of the adsorbates on graphite and graphene can be considered as very similar, we performed our calculations on infinite graphene monolayers using PBC. In the superlattice, graphene layers were separated by 40 Å in the normal direction and represented by orthorhombic unit cells containing two carbon atoms. When modeling the adsorbates on graphene, we used graphene supercells and sampled the Brillouin zone by a 1 × 1 × 1 k-point mesh. The interaction energy E_{inter} of adsorbates with graphite is given by $E_{inter} = E_{tot}$(adsorbates/graphene) − E_{tot}(isolated adsorbates in vacuum) − E_{tot}(graphene). To evaluate the accuracy of the DFT calculations, we have performed the benchmark (see SI). The good agreement with the experimental values indicates that our results with DFT calculations are reasonable.

Considering the London dispersion interaction in van der Waals interaction, we further performed the DFT-D method to estimate the interaction energy of adsorbate with graphite. The DFT-D method really can be considered successfully now on thousands of different systems including inter- as well as intramolecular cases ranging from rare gas dimers to huge graphene sheets.[26−29] In this work, we applied DFT-D3 method (Perdew−Burke−Ernzerhof correlation energy PBE[30] as the DFT functional), in which the an atom-pair wise (atom-triple wise) dispersion correction can be added to the standard Kohn−Sham density functional theory (KS-DFT) energies (and gradient):[26]

$$E_{\text{DFT-D3}} = E_{\text{KS-DFT}} + E_{\text{disp}} \quad (1)$$

with E_{disp} being the sum of the two- and three-body contributions to the dispersion energy:

$$E_{\text{disp}} = E_{(2)} + E_{(3)} \quad (2)$$

The most important two-body term is given at long-range by

$$E_{\text{disp}} = -\frac{1}{2}\sum_{A\neq B}\sum_{n=6,8} s_n \frac{C_n^{AB}}{r_{AB}^n} \quad (3)$$

Here, C_n^{AB} denotes the averaged (isotropic) nth-order dispersion coefficient for atom pair AB, r_{AB}^n is their internuclear distance, and s_n is a functional-dependent scaling factor.

ASSOCIATED CONTENT

Supporting Information

The Supporting Information is available free of charge on the ACS Publications website at DOI: 10.1021/acsnano.5b06666.

Extra benchmark to evaluate the accuracy of the DFT calculations, unit cell of HPB-snowflake, HPB-honeycomb as well as HPB-honeycomb/COR7 results (PDF)
HPB-snowflake crystallographic data CIF
HPB-honeycomb crystallographic data CIF
HPB-honeycomb/COR7 crystallographic data CIF

AUTHOR INFORMATION

Corresponding Authors

*E-mail: zengqd@nanoctr.cn.
*E-mail: kdeng@nanoctr.cn.
*E-mail: limin@ihep.ac.cn.
*E-mail: zhengqy@iccas.ac.cn.

Notes

The authors declare no competing financial interest.

ACKNOWLEDGMENTS

This work was supported by the National Basic Research Program of China (nos. 2011CB933101, 2011CB932501,

DOI: 10.1021/acsnano.5b06666
ACS Nano 2016, 10, 342−348

2013CB934203), National Natural Science Foundation of China (grant nos. 21303208, 51173031, 91127043, 21472029). The Project was also sponsored by the Scientific Research Foundation for the Returned Overseas Chinese Scholars, State Education Ministry (no. Y31Z55), the Start-Up Funding from the Institute of High Energy Physics of the Chinese Academy of Sciences (no. 2011IHEPYJRC504), and the Chinese Academy of Sciences (YZ201318).

REFERENCES

(1) Theobald, J. A.; Oxtoby, N. S.; Phillips, M. A.; Champness, N. R.; Beton, P. H. Controlling Molecular Deposition and Layer Structure With Supramolecular Surface Assemblies. *Nature* **2003**, *424*, 1029−1031.

(2) Stepanow, S.; Lingenfelder, M.; Dmitriev, A.; Spillmann, H.; Delvigne, E.; Lin, N.; Deng, X. B.; Cai, C. Z.; Barth, J. V.; Kern, K. Steering Molecular Organization and Host-Guest Interactions Using Two-Dimensional Nanoporous Coordination Systems. *Nat. Mater.* **2004**, *3*, 229−233.

(3) Xie, L. H.; Ling, Q. D.; Hou, X. Y.; Huang, W. An Effective Friedel-Crafts Postfunctionalization of Poly(N-vinylcarbazole) to Tune Carrier Transportation of Supramolecular Organic Semiconductors Based on *pi*-Stacked Polymers for Nonvolatile Flash Memory Cell. *J. Am. Chem. Soc.* **2008**, *130*, 2120−2121.

(4) Li, M.; Deng, K.; Lei, S. B.; Yang, Y. L.; Wang, T. S.; Shen, Y. T.; Wang, C. R.; Zeng, Q. D.; Wang, C. Site-selective Fabrication of Two-Dimensional Fullerene Arrays by Using a Supramolecular Uemplate At the Liquid-Solid Interface. *Angew. Chem., Int. Ed.* **2008**, *47*, 6717−6721.

(5) Elemans, J. A. A. W.; Lei, S. B.; De Feyter, S. Molecular and Supramolecular Networks on Surfaces: From Two-Dimensional Crystal Engineering to Reactivity. *Angew. Chem., Int. Ed.* **2009**, *48*, 7298−7333.

(6) Cui, K.; Schlutter, F.; Ivasenko, O.; Kivala, M.; Schwab, M. G.; Lee, S. L.; Mertens, S. F. L.; Tahara, K.; Tobe, Y.; Mullen, K.; Mali, K. S.; De Feyter, S. Multicomponent Self-Assembly with a Shape-Persistent N-Heterotriangulene Macrocycle On Au(111). *Chem. - Eur. J.* **2015**, *21*, 1652−1659.

(7) Diez-Perez, I.; Li, Z.; Hihath, J.; Li, J.; Zhang, C.; Yang, X.; Zang, L.; Dai, Y.; Feng, X.; Muellen, K.; Tao, N. Gate-Controlled Electron Transport In Coronenes As a Bottom-Up Approach Towards Graphene Transistors. *Nat. Commun.* **2010**, *1*, 1−5.

(8) Wu, D.; Zhang, H.; Liang, J.; Ge, H.; Chi, C.; Wu, J.; Liu, S. H.; Yin, J. Functionalized Coronenes: Synthesis, Solid Structure, and Properties. *J. Org. Chem.* **2012**, *77*, 11319−11324.

(9) Karlen, S. D.; Reyes, H.; Taylor, R. E.; Khan, S. I.; Hawthorne, M. F.; Garcia-Garibay, M. A. Symmetry and Dynamics of Molecular Rotors In Amphidynamic Molecular Crystals. *Proc. Natl. Acad. Sci. U. S. A.* **2010**, *107*, 14973−14977.

(10) Medeiros, P. V. C.; Gueorguiev, G. K.; Stafström, S. Bonding, Charge Rearrangement and Interface Dipoles of Benzene, Graphene, and PAH Molecules On Au(111) and Cu(111). *Carbon* **2015**, *81*, 620−628.

(11) Shen, Y. T.; Guan, L.; Zhu, X. Y.; Zeng, Q. D.; Wang, C. Submolecular Observation of Photosensitive Macrocycles and Their Isomerization Effects On Host-Guest Network. *J. Am. Chem. Soc.* **2009**, *131*, 6174−6180.

(12) Adisoejoso, J.; Tahara, K.; Okuhata, S.; Lei, S.; Tobe, Y.; De Feyter, S. Two-Dimensional Crystal Engineering: A Four-Component Architecture At a Liquid−Solid Interface. *Angew. Chem., Int. Ed.* **2009**, *48*, 7353−7357.

(13) Li, Y. B.; Deng, K.; Wu, X. K.; Lei, S. B.; Zhao, K. Q.; Yang, Y. L.; Zeng, Q. D.; Wang, C. Molecular Arrays Formed In Anisotropically Rearranged Supramolecular Network With Molecular Substitutional Asymmetry. *J. Mater. Chem.* **2010**, *20*, 9100−9103.

(14) Ghijsens, E.; Cao, H.; Noguchi, A.; Ivasenko, O.; Fang, Y.; Tahara, K.; Tobe, Y.; De Feyter, S. Towards Enantioselective Adsorption In Surface-Confined Nanoporous Systems. *Chem. Commun.* **2015**, *51*, 4766−4769.

(15) Furukawa, S.; Tahara, K.; De Schryver, F. C.; Van der Auweraer, M.; Tobe, Y.; De Feyter, S. Structural Transformation of A Two-Dimensional Molecular Network In Response To Selective Guest Inclusion. *Angew. Chem., Int. Ed.* **2007**, *46*, 2831−2834.

(16) Li, M.; Xie, P.; Deng, K.; Yang, Y. L.; Lei, S. B.; Wei, Z. Q.; Zeng, Q. D.; Wang, C. A Dynamic Study of the Structural Change In the Binary Network In Response To Guest Inclusion. *Phys. Chem. Chem. Phys.* **2014**, *16*, 8778−8782.

(17) Papageorgiou, A. C.; Fischer, S.; Reichert, J.; Diller, K.; Blobner, F.; Klappenberger, F.; Allegretti, F.; Seitsonen, A. P.; Barth, J. V. Chemical Transformations Drive Complex Self-Assembly of Uracil On Close-Packed Coinage Metal Surfaces. *ACS Nano* **2012**, *6*, 2477−2486.

(18) Studener, F.; Müller, K.; Markts, N.; Bulach, V.; Hosseini, M. W.; Stöhr, M. From Hydrogen Bonding To Metal Coordination and Back: Porphyrin-Based Networks On Ag(111). *J. Chem. Phys.* **2015**, *142*, 101926.

(19) Ho, W. Single-Molecule Chemistry. *J. Chem. Phys.* **2002**, *117*, 11033−11061.

(20) Ruben, M.; Payer, D.; Landa, A.; Comisso, A.; Gattinoni, C.; Lin, N.; Collin, J. P.; Sauvage, J. P.; De Vita, A.; Kern, K. 2D Supramolecular Assemblies of Benzene-1,3,5-Triyl-Tribenzoic Acid: Temperature-Induced Phase Transformations and Hierarchical Organization With Macrocyclic Molecules. *J. Am. Chem. Soc.* **2006**, *128*, 15644−15651.

(21) Griessl, S. J. H.; Lackinger, M.; Jamitzky, F.; Markert, T.; Hietschold, M.; Heckl, W. M. Incorporation and Manipulation of Coronene In an Organic Template Structure. *Langmuir* **2004**, *20*, 9403−9407.

(22) Hasegawa, Y.; Avouris, P. Manipulation of the Reconstruction of the Au(111) Surface With the STM. *Science* **1992**, *258*, 1763−1765.

(23) Zhang, R.; Wang, L. C.; Li, M.; Zhang, X. M.; Li, Y. B.; Shen, Y. T.; Zheng, Q. Y.; Zeng, Q. D.; Wang, C. Heterogeneous Bilayer Molecular Structure At a Liquid-Solid Interface. *Nanoscale* **2011**, *3*, 3755−3759.

(24) Becke, A. D. A Multicenter Numerical-Integration Scheme for Polyatomic Molecules. *J. Chem. Phys.* **1988**, *88*, 2547−2553.

(25) Anastassakis, E. Pressure Tuning of Strains and Piezoelectric Fields In Cubic Superlattices and Heterostructures - Linear Effects. *Phys. Rev. B: Condens. Matter Mater. Phys.* **1992**, *46*, 13244−13253.

(26) Grimme, S.; Antony, J.; Ehrlich, S.; Krieg, H. A Consistent and Accurate *ab Initio* Parametrization of Density Functional Dispersion Correction (DFT-D) for the 94 Elements H-Pu. *J. Chem. Phys.* **2010**, *132*, 154104.

(27) Atodiresei, N.; Caciuc, V.; Lazić, P.; Blügel, S. Chemical *versus* van der Waals Interaction: The Role of the Heteroatom In the Flat Absorption of Aromatic Molecules C_6H_6, C_5NH_5, and $C_4N_2H_4$ On the Cu(110) Surface. *Phys. Rev. Lett.* **2009**, *102*, 136809.

(28) Hu, Z. X.; Lan, H. P.; Ji, W. Role of the Dispersion Force In Modeling the Interfacial Properties of Molecule-Metal Interfaces: Adsorption of Thiophene On Copper Surfaces. *Sci. Rep.* **2014**, *4*, 5036.

(29) Medeiros, P. V. C.; Gueorguiev, G. K.; Stafström, S. Benzene, Coronene, and Circumcoronene Adsorbed On Gold, and a Gold Cluster Adsorbed On Graphene: Structural and Electronic Properties. *Phys. Rev. B: Condens. Matter Mater. Phys.* **2012**, *85*, 205423.

(30) Perdew, J. P.; Burke, K.; Ernzerhof, M. Generalized Gradient Approximation Made Simple. *Phys. Rev. Lett.* **1996**, *77*, 3865.

DOI: 10.1021/acsnano.5b06666
ACS Nano 2016, 10, 342−348